AIAA JOURNAL
Vol. 32, No. 8, August 1994

Measurements of Kelvin-Helmholtz Instabilities in a Supersonic Shear Layer

Steven Martens,* Kevin W. Kinzie,* and Dennis K. McLaughlin†
Pennsylvania State University, University Park, Pennsylvania 16802

Experiments have been performed in a new supersonic shear layer facility in which two streams of air are produced in adjacent supersonic sliding block nozzles. Each stream is about 2.5 cm high and 12.5 cm wide. In the present experiments, the high-speed Mach number ranges from 3 to 4 whereas the low-speed stream was held to $M = 1.2$. Running at low-to-moderate Reynolds numbers allows the mixing layer to be studied in the laminar to turbulent transition region as well as under fully turbulent conditions. Low dynamic pressures permit the use of standard hot-wire anemometry without damage to the fragile sensors. Also, the low pressure in the test section permits the use of glow discharge techniques as a means of exciting the shear layer. Initial experiments have included schlieren photography of the flowfield and measurement of the spectral content of the mass-velocity fluctuations in the shear layer for both natural and excited conditions. These observations and measurements show that the glow discharge excitation has a significant effect on the shear layer in terms of growth rate and spectral content of the fluctuations. The increased instability of oblique waves is observed for the higher Mach number conditions.

Nomenclature

a = speed of sound
f = frequency
M = Mach number
$\tilde{m}$ = mass-velocity fluctuation level, $(\rho u)'_{\text{rms}}/\overline{(\rho u)}$
p_{01} = total pressure in high-speed stream
Re = unit Reynolds number based on the high-speed stream properties
St = Strouhal number, $f\delta_\omega/U_1$
U = time mean velocity
u' = fluctuating component of velocity
x = streamwise location, distance from the trailing edge of the splitter plate
δ_ω = local vorticity thickness
ρ = density

Subscripts

c = convective property
e = excitation condition
1 = high-speed stream
2 = low-speed stream

Introduction

SUPERSONIC mixing is a technology essential for further development of projects such as the hypersonic National Aerospace Plane and scramjet engines in general. Supersonic mixing involves two gas streams in which one or both streams have a Mach number greater than one. It has been documented that as the velocity difference between the two streams increases into the supersonic regime, the mixing rate of the two streams and the growth in the thickness of the mixing layer are significantly reduced,[1,2] compared to low-speed shear layers.

Most scramjet engine designs involve some combination of mixing layers in which speed differences exceed the average sound speed. Because of the reduced mixing rate of supersonic shear layers, combustors must be lengthened, resulting in severe weight and drag penalties. For these systems to advance, a means of enhancing the mixing process must be developed. Designers have been handicapped by a lack of understanding of the supersonic shear layer mixing process. Thus, there is a demonstrated need for fundamental research in this area.

An effort to improve the understanding of the fundamental processes which take place in supersonic mixing layers is underway at Penn State University. A new supersonic shear layer facility has been built to study this problem.[3–5] Although the actual combustion process in a real engine takes place at much higher Reynolds numbers, low-to-moderate Reynolds number testing has proven in the past to be a valuable aid in the understanding of high Reynolds number free shear flows.[6,7] At the reduced Reynolds numbers, the viscous stresses suppress the small-scale turbulence. This allows the large-scale instabilities, which are concentrated in a limited frequency range and typically coherent over large distances in the flow, to be characterized with much greater accuracy. In low-speed free shear layers, the dynamics of vortex pairing has been shown to be responsible for the shear layer growth.[8] More complicated three-dimensional effects complete the mixing process as the shear layer grows thicker.[9]

The initial goals of the present study are to investigate the dynamics of the large-scale vortical motions in the supersonic shear layer and to determine what role such large-scale motions play in the mixing process of the layer (as the governing parameters of the flow are varied). In the supersonic shear layer, the large-scale motions grow from instability waves which form early in the shear layer and then, over a relatively long distance, develop into large-scale vortices. One objective of this research is to learn more about the characteristics of these instabilities and how they influence the development of the shear layer. As will be discussed shortly, an important issue concerning these instability waves is how their propagation angle changes as a function of the Mach number difference across the shear layer.

As just noted, operation of the facility in the low-to-moderate Reynolds number range focuses attention on the larger scale motions in the shear layer. There are other advantages to operating at lower Reynolds numbers. The low pressures (and densities) that produce the reduced Reynolds numbers facilitate the use of small hot-wire sensors without concern for damage from high fluctuating dynamic pressures. These hot wires provide convenient and re-

Presented as Paper 92-0177 at the AIAA 30th Aerospace Sciences Meeting, Reno, NV, Jan. 6–9, 1992; received March 10, 1993; revision received March 10, 1994; accepted for publication March 25, 1994.

*Research Assistant, Department of Aerospace Engineering. Student Member AIAA.

†Professor and Head, Department of Aerospace Engineering. Associate Fellow AIAA.

liable measurements of the mass-velocity fluctuations. Also, at the low pressures, a glow discharge system can be implemented to artificially excite the flow.

Another objective of this research is to determine how to increase the mixing in supersonic shear layers. The artificial excitation method, as will be shown, can affect the mean growth of the shear layer and allows some control over the instability waves/turbulence structures. Although much work has been performed on supersonic mixing layers in the past,[1,2,9–14] the combination of the techniques mentioned allows a more detailed study to be made.

Facility Description

Figure 1 shows a schematic of the test section in which two sliding block supersonic nozzles, along with a contoured centerbody, produce adjacent streams of air, merging at the trailing-edge tip. Each of the nozzles may be independently adjusted, allowing the low-speed stream to range from subsonic to Mach 2, while the high-speed stream can range from Mach 2 to Mach 4. Two choked valves upstream of the settling chamber allow separate control for the total pressure of each stream. This facilitates matching the static pressures of each stream as they meet, which ensures that the shear layer will not be deflected by an unbalanced pressure ratio across the shear layer.

The flow passage is 5.5 cm high, 12.5 cm wide, and 75 cm long. The side walls of the test section have optical quality windows allowing schlieren observation to be recorded of the shear layer. The top and bottom walls are flexible and fitted with turnbuckles so that their geometry can be adjusted. This control is necessary to maintain a constant freestream pressure by allowing for the growth of the boundary layers as well as the shear layer itself. Static pressure taps are mounted flush in these walls so that the pressure may be measured throughout the test section. Total pressure probes are located in the settling chamber which, together with the static pressure taps, produce a measurement of the flow Mach number. A total pressure rake can also be placed in the test section, to measure the mean Mach number and velocity profiles across the shear layer.

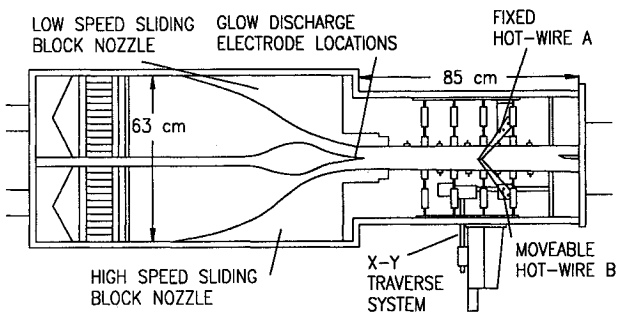

Fig. 1 Schematic of test section.

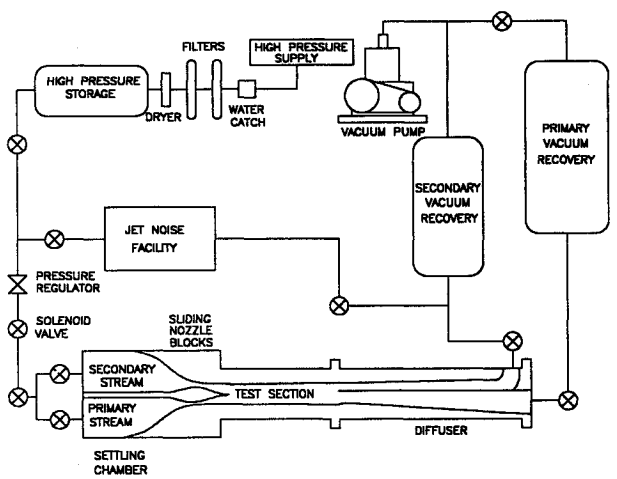

Fig. 2 Schematic of supersonic shear layer facility.

Figure 2 shows a schematic of the facility. Before a run, the two large vacuum recovery tanks and the facility shell are evacuated to below 1 Torr using a vacuum pump. Dried, compressed air is delivered to the facility from a storage tank. When the valve from the compressed air supply is opened, the air flows from the supply tank to the facility. The two upstream control valves create a pressure drop in the flow so that the total pressure of each stream is significantly reduced before entering the settling chamber. The flow then expands through the nozzles, producing supersonic flow in the test section. Total pressures of the high-speed stream range from 0.5 to 2 atm. At the end of the test section the flow is separated and enters a split-stream diffuser. This unique design has increased the pressure recovery and extended run times by 50–100%. For more details of the split-stream diffuser, see Martens.[5]

As noted earlier, low-to-moderate Reynolds numbers are created by running the facility over a range of low-static pressures. Test section pressures of 1/100 of an atmosphere are common. The low-Reynolds-number shear layers in this facility have mass-velocity fluctuations, $\tilde{m} = (\rho u)'_{\text{rms}}/(\rho u)$, on the order of 5% and are characterized by laminar and early transition stages. The moderate Reynolds number shear layers have mass-velocity fluctuations on the order of 20% and correspond to the final stages of transition and conventional fully turbulent flow.

Glow Discharge Excitation System

The low pressure in the test section allows the use of a glow discharge excitation technique. A strip of copper 0.2 cm wide by 10 cm long is attached to, but insulated from, the centerbody, just upstream of the trailing edge on the low-speed side. An ac voltage of 350 V peak-to-peak with a dc offset voltage of −400 V is applied to the copper strip. At sufficiently low pressures, the high voltage ionizes the air, and a local glow is produced from the copper to the aluminum centerbody. The ionization of the air produces a very high temperature in the air next to the surface of the copper strip that is modulated at the ac frequency chosen. This produces density disturbances which perturb the flow. The frequency of the ac voltage can be adjusted to be in the range of the naturally occurring dominant instabilities and produce extremely coherent and discrete waves. In addition to providing a phase reference for the hot-wire measurements, the glow can be used to modify the actual mixing process in the shear layer.

The current configuration of the glow discharge system involves surface mounted copper electrode strips in two arrangements. The first strip is attached normal to the flow direction so as to excite two-dimensional disturbances. The second strip is placed at 45 deg to the flow direction to excite oblique disturbances. For more details on this artificial excitation technique, see Martens.[5]

Instrumentation

Because of the volume of data acquired and the relatively short duration of the experimental runs (8–10 s), an 80386-33 personal computer is used in every phase of data processing from acquisition to final data analysis. A 16-channel analog to digital convertor is controlled by the personal computer to acquire all of the necessary data during a run.

Pressure measurements are made using differential piezoresistive-type pressure transducers. Several different models are used since the pressure in the settling chamber, test section, and diffuser all require different range transducers. A vacuum reference of less than 100-μm Hg is maintained on one side of the transducers. Anemometers consistently provide a frequency response in excess of 50 kHz for the hot-wire probes. The hot wires use a subminiature probe mounted on the end of a brass wedge. When held in place, the probe supports are swept approximately 60 deg backward (from the probe) to reduce the effective flow deflection angle of the leading edge wedge (see Fig. 1). Two probes can be located in the test section with spanwise separation distances of 1.15, 2.77, or 4.96 cm.

Experimental Results

All experimental cases run in the present study involve a supersonic Mach number difference between the two streams, as well as

Table 1 Experimental conditions

Condition	I	II
M_1	3	3.9
M_2	1.2	1.2
$M_{c(\text{theor})}$	0.5	0.64
a_1, *m/s*	203	169
a_2, *m/s*	300	300
P_{01}, Torr	293(96)	700
Re, cm^{-1}	40,000(10,000)	36,000

each individual freestream Mach number exceeding unity. However, the most important parameter for supersonic shear layers appears to be the convective Mach number; the ratio of the convective velocity of turbulence structures (relative to one of the two streams) to the acoustic velocity of the same stream. Papamoschou and Roshko[2] have documented that as the convective Mach number increases, the mixing is decreased. Table 1 summarizes the experimental conditions reported in this work. In all experiments the static pressures of the two streams are matched to within 5%. A limited number of experiments at condition I, $M_1 = 3$, were conducted at a unit Reynolds number of 10,000, shown in parentheses.

The convective Mach number, initially developed by Bogdanoff,[1] provides a reference frame that is traveling with the instability structures and is believed to be the most important compressibility parameter in free shear layers. Papamoschou and Roshko[2] proposed this to be the proper reference frame for the study of supersonic shear layers. The equations used to determine the measured and theoretical convective Mach numbers are as follows:

$$M_{c1} = \frac{U_1 - U_c}{a_1} \qquad M_{c2} = \frac{U_c - U_2}{a_2} \qquad M_{c(\text{theor})} = \frac{U_1 - U_2}{a_1 + a_2}$$

The equation for the theoretical convective Mach number assumes the flow comes to rest isentropically at the stagnation point between two structures (in a coordinate frame moving with the structures). Using this isentropic approximation results in equal theoretical convective Mach numbers $M_{c1} = M_{c2} = M_{c(\text{theor})}$, if the same gas is being used (constant specific heat ratio across the shear layer).

Time Average Measurements

The first qualifying experiments involved test-section static pressure and pitot rake measurements. The purpose behind these experiments was to document the flow in the test section to determine if the design criteria had been met with regard to flow quality, Mach number, and run time. The mean Mach number profile 21 cm downstream of the trailing edge, corresponding to experimental condition I, $M_1 = 3$, is shown in Fig. 3. This profile was determined from an amalgamation of data from several experiments using the 5-pitot-probe rake. At farther upstream locations the wake of the splitter plate is often evident in the mean flow profiles. Mixing has sufficiently spread the two sides of the wake, to eliminate it at this downstream location.

Hot-Wire Measurements

Figures 4a–4c show hot-wire power spectra in terms of both the Strouhal number and the absolute frequency, for three different conditions. These figures exemplify three characteristics of the supersonic shear layer. First, the analysis of Morris et al.[15] predicts that as the shear layer thickens the most dominant instability frequency decreases. The frequency spectra in Figs. 4a and 4b demonstrate this effect for condition I, $M_1 = 3$. Figure 4a resulted from hot-wire data obtained with the probe located at the position of maximum mass-velocity fluctuations, 17 cm downstream of the trailing edge and has a dominant frequency of approximately 23 kHz. The data for Fig. 4b were acquired 33 cm downstream and

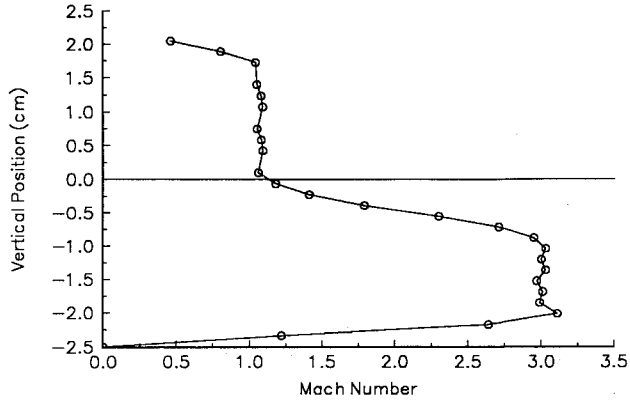

Fig. 3 Mean Mach number profile for condition I, $M_1 = 3$, $x = 21$ cm, and $Re = 40{,}000$/cm.

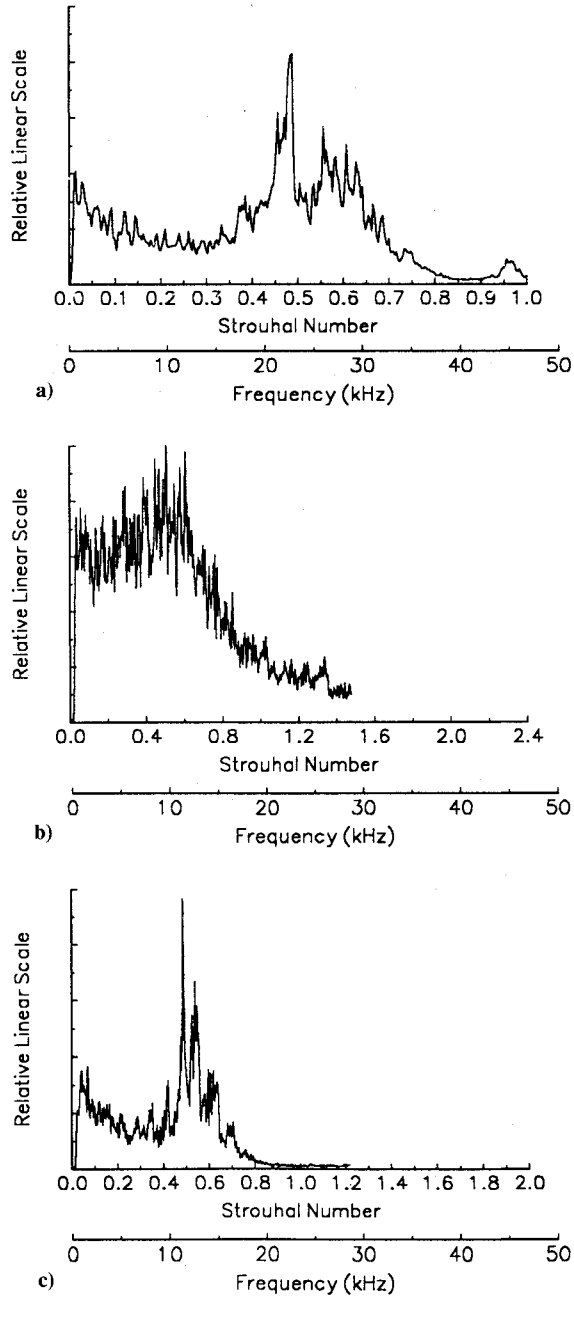

Fig. 4 Natural velocity fluctuation power spectra at condition I, $M_1 = 3$: a) $x = 17$ cm, $Re = 40{,}000$/cm; b) $x = 33$ cm, $Re = 40{,}000$/cm; and c) $x = 43$ cm, $Re = 10{,}000$/cm.

shows a dominant frequency around 12 kHz. Second, Figs. 4b and 4c demonstrate the effect of unit Reynolds number on the power spectra (at approximately the same downstream location) determined from hot-wire signals. The experimental conditions correspond to the Mach numbers of condition I, $M_1 = 3$, with different unit Reynolds numbers. Figure 4b is at a unit Reynolds number of 40,000/cm and shows a very full frequency spectrum with a broad peak centered at around 12 kHz. When the Reynolds number is decreased to 10,000/cm, Fig. 4c, the flow is dominated by a narrow band of frequencies centered around 12 kHz. This shows that as the Reynolds number is decreased, the dominant frequency remains the same, but the spectrum becomes much narrower since most of the energy of the flow is concentrated in the large scales (dominant frequency). This is the expected phenomenon also found in the work of Troutt and McLaughlin[7] who measured instabilities in a moderate Reynolds number axisymmetric shear layer. Hot-wire power spectra with these characteristics are common for supersonic shear layers with this Mach number and Reynolds number range. The multiple peak structures are believed to result from an interaction of the large-scale instabilities with the lower frequency facility resonances that are particularly evident in Figs. 4a and 4c. Finally, when looking at the Strouhal number axes, all three figures have a dominant peak at a Strouhal number of about 0.5. This collapsing of the Strouhal number spectra is the result of the shear layer thickening as it develops downstream (and the corresponding increase of all length scales), whereas the dominant frequency decreases proportionally.

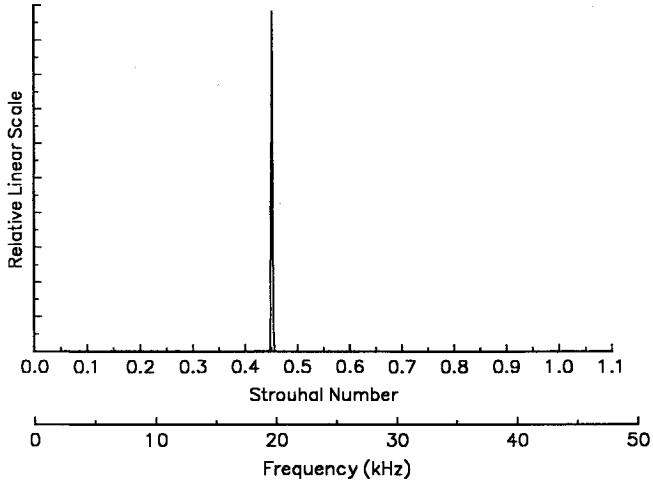

Fig. 5 Hot-wire power spectrum excited at 20 kHz, with the two-dimensional electrode, condition I, $M_1 = 3$, $x = 17$ cm, and $Re = 40{,}000/$ cm.

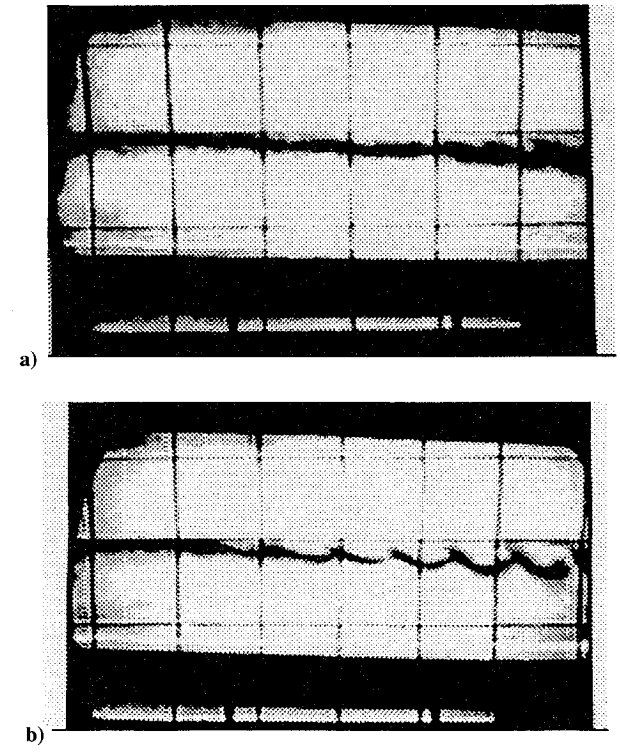

Fig. 6 Schlieren photograph of condition I, $M_1 = 3$, beginning 8 cm downstream of the trailing edge; each grid is 2 × 2 cm: a) natural shear layer and b) excited shear layer, $f_e = 33$ kHz, two-dimensional electrode).

Excited Shear Layer Measurements

The hot-wire power spectrum of Fig. 5 is recorded at the same conditions as the spectrum of Fig. 4a (condition I, $M_1 = 3$), except that for the case of Fig. 5, the shear layer is excited by the two-dimensional oscillating glow discharge electrode at a frequency of 20 kHz ($St = 0.45$). The excitation frequency is equal to the most dominant frequency at a location early in the shear layer development. Excitation with the oblique, three-dimensional electrode produces the same discrete peak in the spectrum. The normalized mass-velocity fluctuations for the unexcited shear layer are $\tilde{m} = 0.19$, whereas for the two dimensionally excited shear layer $\tilde{m} = 0.26$, showing an increase in fluctuations when the shear layer is excited. The effect of the glow can also be seen in oscilloscope traces of the hot-wire signal and the glow excitation signal. When both signals are displayed simultaneously, a normally incoherent and jumbled natural hot-wire signal phase locks perfectly with the excitation signal.

Figure 6 shows schlieren photographs of the natural shear layer (Fig. 6a) and the shear layer excited (two-dimensional electrode) at approximately 33.3 kHz (Fig. 6b), for condition I ($M_1 = 3$). Flow is from left to right and the high-speed stream is on the bottom. The

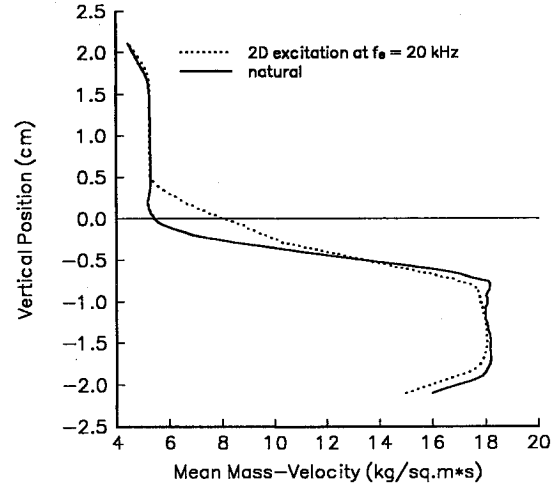

Fig. 7 Mean mass-velocity profile, condition I, $M_1 = 3$, $x = 21$ cm, and $Re = 40{,}000$/cm.

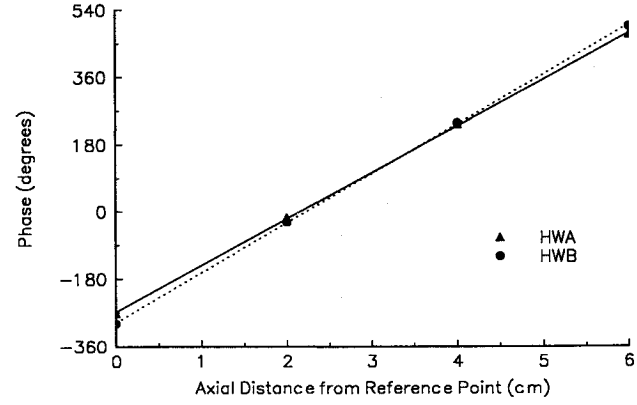

Fig. 8 Phase angle vs axial distance from reference point, condition I, $M_1 = 3$, two-dimensional electrode, spanwise separation 4.96 cm.

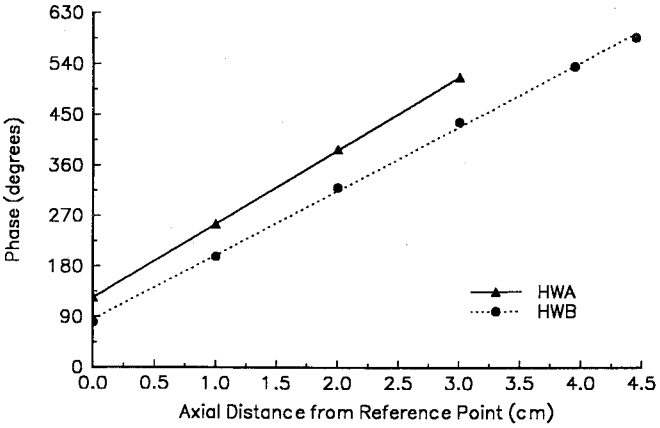

Fig. 9 Phase angle vs axial distance from reference point, condition II, $M_1 = 3.9$, three-dimensional electrode, spanwise separation 4.96 cm.

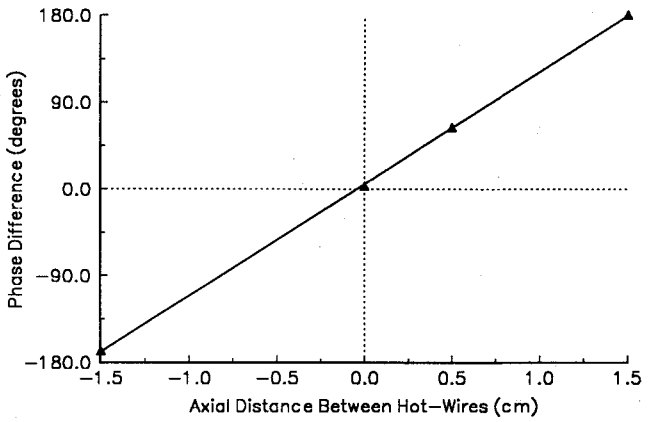

Fig. 10 Phase difference vs axial separation distance between hot wires separated by a spanwise distance 1.15 cm, condition II, $M_1 = 3.9$, three-dimensional electrode.

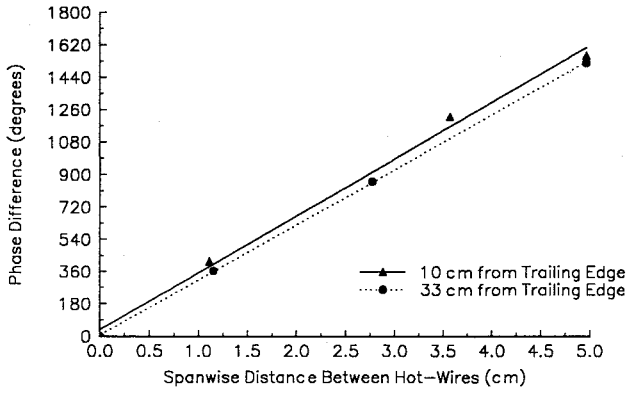

Fig. 11 Phase difference vs spanwise separation distance between hot wires located at the same axial position, condition II, $M_1 = 3.9$, three-dimensional electrode.

grid spacings in the pictures are 2 × 2 cm. The photograph of the excited shear layer was taken by synchronizing a strobe light with the glow excitation signal. A frequency dividing circuit is used to divide the excitation frequency by 16 to lower the strobing frequency to within the operating limits of the strobe light. Large-scale structures are clearly visible in the excited case.

Mean mass-velocity profiles have also been measured for excited and unexcited conditions. Figure 7 shows these profiles measured 21 cm downstream of the trailing edge, for experimental Condition I ($M_1 = 3$). The excited ($f_e = 20$ kHz, two-dimensional electrode) profile is thicker and fuller than the unexcited profile. Evidence of the trailing-edge wake is also visible in the natural shear layer but is not present in the excited case. This shows that artificial excitation at a dominant natural frequency enhances shear layer growth under these conditions.

Phase Measurements

$M_1 = 3$ (Condition I)

As demonstrated in the previous section, hot-wire measurements show that the instability waves can be made to phase lock with the glow discharge excitation signal and create very coherent waves in the shear layer. Therefore, cross-spectral analysis between the excitation signal and a single hot-wire signal (or between two hot-wire signals) in an excited shear layer allow relative phase measurements of the instability waves to be made. For experimental condition I, $M_1 = 3$, Fig. 8 shows how the phase changes between the two-dimensional excitation signal and a single hot-wire signal as the probe is moved downstream, beginning approximately 23 cm downstream of the trailing edge. Two such groups of experiments are made using two probes (A and B) separated by a distance in the spanwise direction of 4.96 cm. The two-dimensional excitation frequency is 20 kHz. It is important to note here that the interpretation of Strouhal number changes in excited

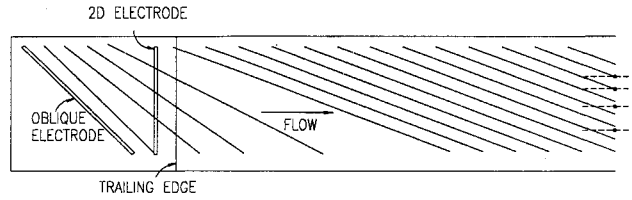

Fig. 12 Schematic of hot-wire positions and wavefronts for condition II, $M_1 = 3.9$, shear layer.

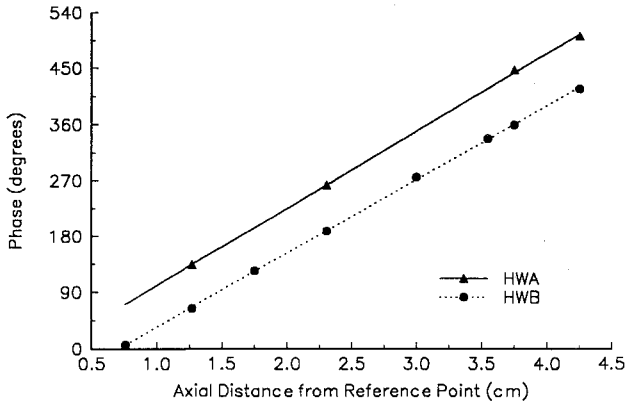

Fig. 13 Phase angle vs axial distance from reference point, condition II, $M_1 = 3.9$, two-dimensional electrode, spanwise separation 4.96 cm.

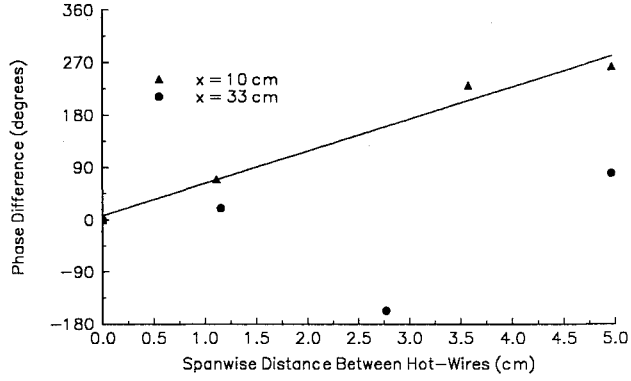

Fig. 14 Phase difference vs spanwise separation distance between hot wires located at the same axial position, condition II, $M_1 = 3.9$, two-dimensional electrode.

Table 2 Measured wave angles and wavelengths

M_1	3	3.9	3.9	3.9
Effective electrode orientation, deg	0	0	0	64
Excitation frequency, kHz	20	20	20	20
Downstream location, cm	10 and 26	10	33	10 and 33
Axial wavelength, cm	2.8	3.0	3.0	3.0
Spanwise wavelength, cm	n/a	6.5	—	1.18
Wave angle, deg	0	25	—	69

shear layers since the frequency has become a constant. Therefore, the Strouhal number continuously changes throughout the test section since the shear layer is thickening whereas the frequency remains constant.

Since phase is linearly related to the wavelength, the slope of these lines yield the streamwise wavelength of the turbulence structures, i.e., the axial size of the large-scale structures (wavelength = 360 deg/m, where m is the slope of the line). Both measurements show the waves to be approximately 2.8 cm long. Also, note that at both spanwise locations, the phase of the instability waves with respect to the excitation signal is approximately the same. This implies that the waves remain two dimensional, oriented normal to the flow, as they travel downstream and convect by the hot-wire probes.

M_1 = 3.9 (Condition II)

The results of the three dimensionally excited shear layer will be discussed prior to those of the two dimensionally excited shear layer at this higher speed condition. This is because the results in the two-dimensional case are rather ambiguous and difficult to explain. Present theory and observations indicate that as the convective Mach number of the shear layer increases, the amplification of oblique instability waves is expected. This has been predicted by Morris et al.[15] and Gropengieser[16] among others and is discussed in the interpretation of supersonic shear layer observations of Clemens and Mungal.[12] To investigate this possibility, similar phase measurements (as those shown in Fig. 8) have been performed using the oblique excitation electrode, oriented at 45 deg to the flow direction. Measurements of this type are performed in the M_1 = 3.9 shear layer (experimental condition II) excited at f_e = 20 kHz. Since the oblique electrode starts at the exit of the low-speed side of the nozzle and extends upstream toward the throat, there is a velocity differential along the length of the electrode. As a result, by the time the entire wave has convected off the centerbody, into the shear layer, it is at a steeper angle than 45 deg. Taking into account these velocity differences, the actual excitation angle is estimated to be 64 deg. Figure 9 shows the phase difference between the three-dimensional excitation signal and hot-wire signals A and B as the probes are moved downstream, beginning approximately 33 cm downstream from the trailing edge. The spanwise separation distance between the wires is 4.96 cm. As might be expected, the hot-wire signals show a definite phase difference, although each line results in the same axial wavelength of 3.0 cm.

Figure 10 shows the phase difference between two hot wires separated by a spanwise distance of 1.15 cm as the axial distance between them is changed. Note that by correlating the two hot-wire signals directly, rather than correlating each of them with the glow signal, the phase difference between the two can be determined directly by looking at the y intercept of Fig. 10. For this spanwise separation, the phase difference is seen to be approximately 0 deg (when the hot wires are at the same axial location). The axial wavelength determined from this graph is again 3.0 cm.

Figure 11 shows the phase difference between two hot wires as a function of spanwise separation distance for two axial positions, 10 and 33 cm downstream of the trailing edge. The slope of each line yields a spanwise wavelength of 1.18 cm. Together with the measured axial wavelength of 3.0 cm, this gives a wave angle of 69 deg at both downstream locations. This result seems very reliable, with consistent measurements at two different axial locations in the shear layer. The initial point (0, 0) is included in Fig. 11

Table 3 Measured and theoretical convective Mach numbers

M_1, M_2	$U_{c(\text{meas})}$, m/s	$U_{c(\text{theor})}$, m/s	M_{c1}, M_{c2} measured	$M_{c(\text{theor})}$
3, 1.2	475	502	0.24, 0.67	0.5
3.9, 1.2	600	556	0.35, 0.8	0.64

since two hot wires at the same position will have zero phase difference. The data points for Fig. 11 are obtained from the y intercept of a phase diagram such as that in Fig. 10, that is, the value of phase difference for zero axial separation distance between the two hot wires. If the spanwise wavelength of the instability wave is larger than the separation distance between hot wires, integer multiples of 2π must be added to the measured phase.

Figure 12 is a sketch of the wave fronts measured at the downstream locations around x = 33 cm, showing (dotted lines) the locations of the hot-wire probes for the phase measurements used to determine the wave fronts. This figure shows that in some cases the separation distance between probes is less than the spanwise wavelength and thus integer multiples of 2π must be added, as discussed previously. It is difficult at present to make a precise interpretation of this result since the actual orientation of excitation is about 64 deg and the oblique convection angle of the measured instability wave is 69 deg. An error analysis was performed using the data required to calculate this convection angle resulting in an experimental error of ±6 deg. The remaining uncertainty is whether 69 deg is a natural wave angle in the shear layer, or if it is simply forced by the orientation of the excitation electrode. Further measurements with different electrode orientations are planned to resolve this issue. Such results from three-dimensional excitation have a consistency with similar kinds of measurements made by Kendall[17] in a Mach 4.5 flat plate boundary layer. However, to the authors' knowledge, this is the first time oblique instability waves have been quantitatively measured in a supersonic shear layer.

Additional information regarding three-dimensional waves is seen in phase measurements of the M_1 = 3.9 (condition II) shear layer with two-dimensional electrode excitation. The excitation frequency is 20 kHz and the axial position is 33 cm downstream of the splitter plate trailing edge. In comparison with the M_1 = 3 (condition I) phase data (Fig. 8), the results shown in Fig. 13 are similar except, at the higher Mach number, the two spanwise locations are seen to be consistently out of phase by approximately 80 deg. This implies that at the higher convective Mach number, an artificially excited two-dimensional wave skews toward a more oblique orientation. Again, the axial wavelength is found to be 3.0 cm from this figure.

This data base is expanded by repeating the measurements of Fig. 13 with different probe spacings, producing data like those shown in Fig. 10, now for the two-dimensional excitation case. The results of such experiments are summarized in Fig. 14. Again, there are data sets corresponding to the downstream locations of 10 and 33 cm. Unlike the similar graph for the oblique wave excitation (Fig. 11, phase difference vs spanwise distance between hot wires), we see an inconsistent trend in these data. At the upstream location a linear phase relation is again found, and a spanwise wavelength of 6.5 cm results corresponding to a wave angle of 25 deg. The data for the downstream location, however, does not show a linear relationship between phase difference and hot-wire separation distance. A possible reason for this anomaly is that through the test section, originally two-dimensional waves undergo a skewing process to oblique orientations. It is also possible that during the skewing process the simple waves undergo some type of dislocation resulting in waves traveling in two oblique directions, which the two probes cannot resolve. This situation would produce a phase diagram that is not a straight line but switches slope somewhere across the test section. One could assume that the planar Mie scattering observations showing highly three-dimensional structures by Clemens and Mungal[12] would produce similar (but probably even more complicated) phase relationships. The conclusion reached in the case of two-dimensional excitation for the Mach 4 shear layer is that a very complicated situation arises, and all the questions have not yet been answered.

Table 2 summarizes the results of the phase data for the different Mach number and electrode orientation conditions.

Convective Mach Number Measurements

Table 3 provides a comparison of the measured and theoretical convective Mach numbers achieved in this facility. The measured values of U_c were determined from the (measured) frequency and axial wavelength of the instability structure, calculated from phase diagrams, discussed in the previous sections. The measured wavelengths were also corroborated in many cases with schlieren photographs similar to Fig. 6b. It is clear that the isentropic model used to calculate the theoretical convective Mach number is not precise and tends to lose accuracy as the convective Mach number increases. Papamoschou[18] proposes two possible reasons for the failure of the isentropic model as the convective Mach number increases and the flow becomes highly compressible. First, shock waves may form on the structures altering the stagnation pressure. Second, the structures may become highly three dimensional, as we have just shown with the data already given. Either one of the situations would nullify the two dimensionally based isentropic model.

Conclusions

A preliminary characterization of large-scale instabilities/turbulence structures in a supersonic free shear layer has been conducted. A method of artificially exciting the shear layer using an oscillating glow discharge technique has been developed. It has been shown that this excitation will significantly concentrate the fluctuations to the spectral band around the frequency of interest. The excitation raises the level of fluctuation energy and can cause the shear layer to spread more rapidly.

Detailed phase measurements with hot wires in the flowfield excited by two-dimensional and oblique glow discharge electrodes produce relatively accurate estimates of instability phase fronts. At the higher Mach number ($M_1 = 3.9$) condition, evidence of the increased instability of the oblique waves is seen. Glow excitation facilitates the measurement of oblique instability waves/turbulence structures in the shear layer. Although, this situation has been predicted some time ago, this is the first detailed experimental verification the authors' are aware of.

The unique capabilities of this facility lend themselves to the study of the supersonic mixing problem in a way never before possible. The ability to quantitatively analyze the flowfield using hotwire anemometry is very important. The glow discharge has proven to have an effect on the shear layer. With continued development, the glow excitation may even be used to enhance the mixing process in the shear layer. Helium, added to the high-speed side, will boost the convective Mach number easily into the supersonic range. The type of research being performed in this facility will be important to further advance our understanding of supersonic free shear layers.

Acknowledgments

This work was supported by the Office of Naval Research, Grant NN0014-88-K-0242, monitored by S. G. Lekoudis and L. P. Purtell. Additional support from J. M. Tishkoff of the Air Force Office of Scientific Research is also gratefully acknowledged. The authors wish to thank P. J. Morris for his continuing discussions and P. Carpenter for his contributions in the split-stream diffuser design. Fellow graduate students C. Hackett, N. Kamvissis, A. Vaddempudi, and W. D. Barron provided significant help with the facility assembly.

References

[1]Bogdanoff, D. W., "Compressibility Effects in Turbulent Shear Layers," *AIAA Journal*, Vol. 21, No. 6, 1983, pp. 926, 927.

[2]Papamoschou, D., and Roshko, A., "The Compressible Turbulent Shear Layer: An Experimental Study," *Journal of Fluid Mechanics*, Vol. 197, Dec. 1988, pp. 453–477.

[3]Hackett, C., "Design and Analysis of a Low Reynolds Number Supersonic Shear Layer Facility," M.S. Thesis, Department of Aerospace Engineering, Pennsylvania State Univ., University Park, PA., Dec. 1989.

[4]Kinzie, K. W., "Measurements of the Large-Scale Instabilities in a Low Reynolds Number Two-Stream Supersonic Shear Layer," M.S. Thesis, Department of Aerospace Engineering, Pennsylvania State Univ., University Park, PA, Jan. 1991.

[5]Martens, S., "Enhancements to a Low Reynolds Number, Two-Stream Supersonic Shear Layer Facility," M.S. Thesis, Department of Aerospace Engineering, Pennsylvania State Univ., University Park, PA, May 1992.

[6]Morrison, G. L., and McLaughlin, D. K., "Instability Process in Low Reynolds Number Supersonic Jets," *AIAA Journal*, Vol. 18, No. 7, 1980, pp. 793–800.

[7]Troutt, T. R., and McLaughlin, D. K., "Experiments on the Flow and Acoustic Properties of a Moderate Reynolds Number Supersonic Jet," *Journal of Fluid Mechanics*, Vol. 116, March 1982, pp. 233–256.

[8]Winant, C. D., and Browand, F. K., "Vortex Pairing: The Mechanism of Turbulent Mixing at Moderate Reynolds Numbers," *Journal of Fluid Mechanics*, Vol. 63, Pt. 2, 1974, pp. 237–255.

[9]Dimotakis, P. E., "Turbulent Free Shear Layer Mixing," AIAA Paper 89-0262, Jan. 1989.

[10]Demetriades, A., and Brower, T., "Experiments on the Free Shear Layer Between Two Supersonic Streams," AIAA Paper 90-0710, Jan. 1990.

[11]Hall, J. L., Dimotakis, P. E., and Rosemann, H., "Experiments in Non–Reacting Compressible Shear Layers," AIAA Paper 91-0629, Jan. 1991.

[12]Clemens, N. T., and Mungal, M. G., "Two- and Three-Dimensional Effects in the Supersonic Mixing Layer," *AIAA Journal*, Vol. 30, No. 4, 1992, pp. 973–981.

[13]Samimy, M., Reeder, M. F., and Elliott, G. S., "Compressibility Effects on Large Structures in Free Shear Flows," *Physics of Fluids A*, Vol. 4, No. 6, 1992, pp. 1251–1258.

[14]Shau, Y. R., Dolling, D. S., and Choi, K. Y., "Organized Structure in a Compressible Turbulent Shear Layer," *AIAA Journal*, Vol. 31, No. 8, 1993, pp. 1398–1405.

[15]Morris, P. J., Giridharan, M. G., and Lilley, G. M., "On the Turbulent Mixing of Compressible Free Shear Layers," *Proceedings of the Royal Society of London*, Vol. 431, No. 1882, 1990, pp. 219–243.

[16]Gropengieser, H., "Study on the Stability of Boundary Layers and Compressible Fluids," NASA TT F-12,786, May 1969.

[17] Kendall, J. M., "Supersonic Boundary Layer Stability Experiments," *Proceedings of the Boundary Layer Transition Study Group Meeting*, Vol. II, The Aerospace Corporation, Aerospace Rept. TR–0158, (S3816-63)-1, 1967.

[18]Papamoschou, D., "Structure of the Compressible Turbulent Shear Layer," *AIAA Journal*, Vol. 29, No. 5, 1991, pp. 680, 681.